Med Chem Res
DOI 10.1007/s00044-015-1321-0

MEDICINAL CHEMISTRY RESEARCH

ORIGINAL RESEARCH

The antimitotic pyrimido[4,5-*c*]quinolin-1(2*H*)-one scaffold: probing substituents at position 3

Kamel Metwally · Harris Pratsinis · Dimitris Kletsas

Received: 22 August 2014 / Accepted: 29 December 2014

Abstract As a continuation of our efforts to optimize the antimitotic effect of our pyrimido[4,5-*c*]quinolin-1(2*H*)-one scaffold, we were interested in exploring the SAR of substituents at position 3 of this fused ring system. Target compounds **2a–r** having substituents with diverse electronic and steric characteristics at the 3-phenyl ring were synthesized and tested for in vitro cytotoxicity against lung fibrosarcoma HT-1080 and colon adenocarcinoma HT-29 human cancer cell lines using the widely accepted MTT assay. Most of the compounds displayed cytotoxic effects in the low micromolar range. Clear-cut SAR conclusions were drawn from the available biological data. Generally, o-substitution results in a marked decrease or complete loss of cytotoxicity. Multimethoxy substitution in this particular position does not contribute to the cytotoxic effect but leads to cytotoxic selectivity for HT-1080 versus HT-29 cells. Interestingly, the best position for cytotoxicity of a halogen was the p-position, whereas m-substitution was the most favourable within the methyl/methoxy series. To confirm the mechanism of action previously identified for our closely related analogues, the most cytotoxic compounds were evaluated for their effects on cell cycle progression and tubulin polymerization. All compounds tested were found to arrest HT-1080 cells in the G2/M phase of the cell cycle and inhibit tubulin polymerization in a similar fashion to colcemid which is a known tubulin polymerization inhibitor.

Graphical Abstract

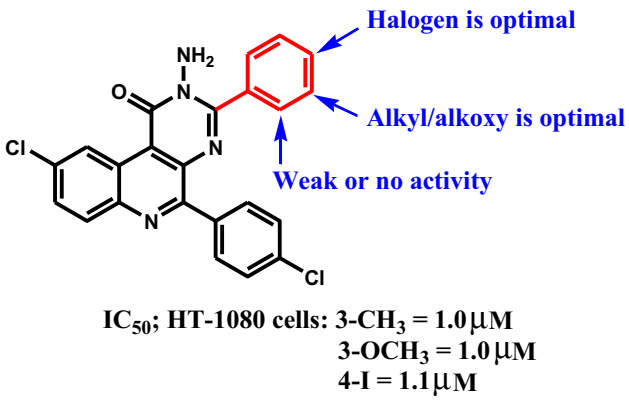

Keywords Cytotoxic agents · Anticancer · Antimitotic · Pyrimido[4,5-*c*]quinolin-1(2*H*)-ones

Introduction

Microtubules, simply polymers of alternating α- and β-tubulin subunits, are prominent components in the cytoskeleton (Zhou and Giannakakou, 2005). Not only microtubules play a crucial role in mitosis and cell replication, but they are also involved in other important cellular activities such as cell movement, cell shape, and transport of organelles inside the cell (Nogales, 2001; Downing, 2000, Sorger *et al.*, 1997; Honore *et al.*, 2005). Chemical substances, natural or synthetic, which have the ability to bind tubulin,

Electronic supplementary material The online version of this article (doi:10.1007/s00044-015-1321-0) contains supplementary material, which is available to authorized users.

K. Metwally (✉)
Department of Medicinal Chemistry, Faculty of Pharmacy, Zagazig University, Zagazig, Egypt
e-mail: kametwally@hotmail.com

H. Pratsinis · D. Kletsas
Laboratory of Cell Proliferation and Ageing, Institute of Biology, National Centre of Scientific Research "Demokritos", Athens, Greece

Published online: 25 January 2015

interfere with microtubule dynamics by either promoting or inhibiting tubulin polymerization and hence microtubule assembly (Zhou and Giannakakou, 2005; Jordan and Wilson, 2004). Drugs which interfere with microtubule dynamics are called antimitotic agents. These drugs can be broadly categorized into two groups, namely tubulin polymerization promoters and inhibitors. The taxanes such as paclitaxel and docetaxel typify tubulin polymerization promoters, whereas colchicine, combretastatins, and the vinca alkaloids typify tubulin polymerization inhibitors. It is well documented that tubulin-binding drugs induce mitotic catastrophe followed by apoptotic cell death by arresting cells in the G2/M phase of cell cycle (Honore *et al.*, 2005; Dumontet and Jordan, 2010; Amos, 2011). In addition, these drugs were reported to have clinically relevant antiangiogenic and vascular-disrupting properties, which were attributed to their ability to inhibit endothelial cell proliferation, migration, and tube formation (Schwartz, 2009). Given such importance in cancer pathophysiology, tubulin remains one of the most attractive targets in cancer chemotherapy.

Our interest in pursuing anti-tubulin drugs had previously led us to the discovery of pyrimido[4,5-*c*]quinolin-1(2*H*)-ones as an interesting scaffold for antimitotic anticancer agents (Metwally *et al.*, 2007a). The first set of target compounds with this fused ring system and having a 2-amino substituent showed in vitro cytotoxic activity at the low micromolar level against a panel of human cancer cell lines. Initial mechanistic studies led to the identification of tubulin as the biological target of this class of compounds (Metwally *et al.*, 2007a). Subsequently, we started a systematic structure–activity relationship study for the sake of having deep insight into structural determinants of cytotoxic activity and fine tuning the antimitotic effect. Some important conclusions were drawn from our previous SAR investigations. At position 2, substituted phenyl analogues were cytotoxic and showed cytotoxic selectivity for certain cancer cell lines but were generally less potent than their 2-amino counterparts (Metwally *et al.*, 2007b, 2013). This directed us to focus on studying 2-aminopyrimido[4,5-*c*]quinolin-1(2*H*)-ones. Among quinoline benzenoid ring substituents tested, chloro, iodo, or methoxy groups at C-9 were generally shown to give the most potent cytotoxic compounds. Substantially lower cytotoxic activity was displayed by 7-chloro versus their 9-chloro counterparts in all cell lines tested (Metwally *et al.*, 2010).

A few substituents at position 3 were preliminarily explored in a previous study (Metwally *et al.*, 2007a). It was concluded that a 3-phenyl ring significantly enhanced cytotoxicity when compared to a 3-methyl group. Moreover, p-chloro substitution was found to further enhance cytotoxic activity (Fig. 1). In this context, the aim of this investigation was primarily to examine, in depth, the effect of substitution at position 3 of our pyrimido[4,5-*c*]quinolin-1(2*H*)-one antimitotic scaffold for the purpose of formulating a comprehensive structure–activity relationship. To achieve this goal, the 3-phenyl ring was substituted at different positions with atoms and groups of diverse electronic and steric properties. Guided by our previous SAR data, we fixed substituents at positions 5 and 9 as 4-chlorophenyl and chloro, respectively.

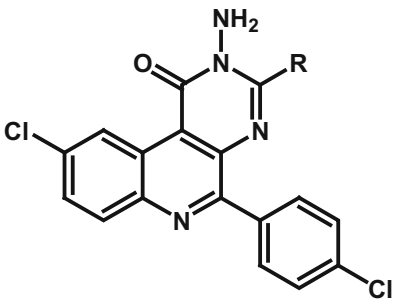

	IC_{50} (μM)	
	HT-1080	HT-29
CH_3	34.3 (± 7.2)	52.0 (± 24.0)
C_6H_5	2.90 (± 0.58)	4.68 (± 0.79)
4-Cl-C_6H_4	1.23 (± 0.22)	1.97 (± 0.007)

Fig. 1 Previous cytotoxicity data of pilot position 3 probes

Materials and methods

Chemistry

Melting points were determined on a Barnstead Electrothermal 9100 melting point apparatus and are uncorrected. ^{1}H-NMR spectra were recorded in DMSO-d_6 on a Varian Mercury 300-MHz spectrometer. Chemical shifts were expressed in parts per million (ppm) downfield from tetramethylsilane (TMS). ^{13}C-NMR spectra were recorded at 75 MHz in DMSO-d_6 on a Bruker 400-MHz spectrometer. Elemental analyses (C, H, N) were performed at the Microanalytical Unit, Cairo University, Cairo, Egypt. All compounds were routinely checked by thin-layer chromatography (TLC) on aluminium-backed silica gel plates. All solvents were dried by standard methods. Compounds **1** and **2d** were reported previously (Metwally *et al.*, 2007a).

Synthetic route to the target compounds is outlined in Scheme 1. The starting 3-amino-6-chloro-2-(4-chlorophenyl)quinoline-4-carboxylic acid (**1**) was synthesized from 5-chloroisatin and 4-chlorophenacylamine hydrochloride under the basic conditions of the Pfitzinger reaction as previously reported (Metwally *et al.*, 2007a). Condensation of the starting acid with the appropriate benzoyl chlorides in pyridine at room temperature afforded the intermediate lactones which were used directly for the synthesis of the desired target compounds (**2a–r**) in fair yields through condensation with hydrazine hydrate in 2-methoxyethanol under reflux

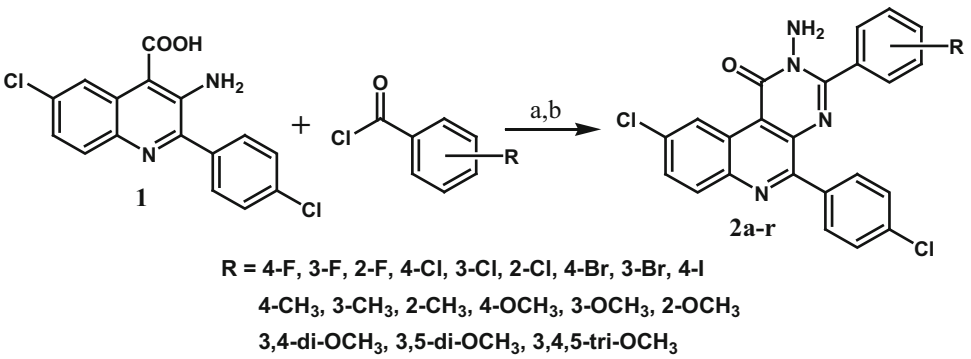

Scheme 1 Reagents and conditions: *a* pyridine, 0 °C to room temperature, 16 h and *b* hydrazine hydrate 99 %, 2-methoxyethanol, reflux, 24 h

conditions. All the target compounds in the present investigation were structurally elucidated by ^{1}H-NMR, EIMS spectral data, and elemental analysis.

*General procedure for 2-amino-9-chloro-5-substitutedarylpyrimido[4,5-c]quinolin-1(2H)-ones (**2a–r**)*

A solution of the 3-amino-6-chloro-2-(4-chlorophenyl)quinolone-4-carboxylic acid (**1**; 10 mmol) in pyridine was cooled in an ice bath and the appropriate benzoyl chloride (25 mmol) was added in a dropwise manner while stirring. After addition was complete, the reaction mixture was allowed to stir at room temperature for 16 h. Cold ethanol was added to the reaction mixture, and the precipitated solid was filtered, washed with water and ethanol, and dried. The solid was suspended in 2-methoxyethanol (40 mL), hydrazine hydrate (99 %; 4 mL) was added, and the mixture was heated at reflux for 24 h. The precipitated solid was filtered, washed with ethanol, dried, and recrystallized from the appropriate solvent.

*2-Amino-9-chloro-5-(4-chlorophenyl)-3-(4-fluorophenyl) pyrimido[4,5-c]quinolin-1(2H)-one (**2a**)*

Yield 55 %, mp 297–298 °C (DMF); ^{1}H-NMR (DMSO-d_6) δ: 6.10 (s, 2H, NH_2), 7.35–7.40 (m, 2H, 3-Phenyl-H), 7.60 (d, 2H, $J = 6.33$ Hz, 5-phenyl-H), 7.92 (dd, 1H, $J = 6.6$, 1.65 Hz, C_8-H), 8.02–8.05 (m, 2H, 3-phenyl-H), 8.15 (d, 2H, $J = 6.33$ Hz, 5-phenyl-H), 8.22–8.24 (m, 1H, C_7-H), 9.74 (d, 1H, $J = 1.92$ Hz, C_{10}-H). EIMS m/z 450 (M^+). Anal. calcd for $C_{23}H_{13}Cl_2FN_4O$: C, 61.21; H, 2.90; N, 12.42. Found: C, 60.99; H, 3.01; N, 12.68.

*2-Amino-9-chloro-5-(4-chlorophenyl)-3-(3-fluorophenyl) pyrimido[4,5-c]quinolin-1(2H)-one (**2b**)*

Yield 58 %, mp 274–276 °C (DMF); ^{1}H-NMR (DMSO-d_6) δ: 6.07 (s, 2H, NH_2), 7.48–7.51 (m, 1H, Ar–H, 3-phenyl-H), 7.56–7.59 (m, 2H, 3-phenyl-H), 7.74–7.75 (m, 1H, 3-phenyl-H), 7.90–7.92 (m, 2H, C_8-H, 5-phenyl-H), 8.11–8.27 (Complex m, 4H, 5-phenyl-H, C_7-H), 9.72–9.73 (m, 1H, C_{10}-H). EIMS m/z 450 (M^+). Anal. calcd for $C_{23}H_{13}Cl_2FN_4O$: C, 61.21; H, 2.90; N, 12.42. Found: C, 60.98; H, 2.96; N, 12.07.

*2-Amino-9-chloro-5-(4-chlorophenyl)-3-(2-fluorophenyl) pyrimido[4,5-c]quinolin-1(2H)-one (**2c**)*

Yield 50 %, mp 254–257 °C (DMF); ^{1}H-NMR (DMSO-d_6) δ: 5.93 (s, 2H, NH_2), 7.35–7.39 (m, 2H, 3-phenyl-H), 7.55 (d, 2H, $J = 6.33$ Hz, 5-phenyl-H), 7.61–7.62 (m, 1H, 3-phenyl-H), 7.71–7.75 (m, 1H, 3-phenyl-H), 7.88–7.94 (m, 1H, C_8-H), 8.09 (d, 2H, $J = 6.33$ Hz, 5-phenyl-H), 8.19 (d, 1H, $J = 6.6$ Hz, C_7-H), 9.65–9.70 (m, 1H, C_{10}-H). EIMS m/z 450 (M^+). ^{13}C-NMR (DMSO-d_6) δ: 115.55, 115.76, 118.34, 123.07, 124.14, 124.39, 124.42, 124.85, 127.83, 130.05, 131.16, 131.19, 131.70, 132.51, 132.82, 133.95, 134.50, 136.39, 140.76, 143.01, 154.21, 157.04, 160.88. Anal. calcd for $C_{23}H_{13}Cl_2FN_4O$: C, 61.21; H, 2.90; N, 12.42. Found: C, 60.96; H, 2.97; N, 12.71.

*2-Amino-9-chloro-5-(4-chlorophenyl)-3-(3-chlorophenyl) pyrimido[4,5-c]quinolin-1(2H)-one (**2e**)*

Yield 61 %, mp > 300 °C (DMF); ^{1}H-NMR (DMSO-d_6) δ: 6.09 (s, 2H, NH_2), 7.54–7.63 (m, 3H, 3-phenyl-H, 5-phenyl-H), 7.88 (d, 1H, $J = 5.22$ Hz, C_8-H), 7.93–7.95 (m, 1H, 3-phenyl-H), 8.02–8.03 (m, 2H, 3-phenyl-H), 8.14 (d, 2H, $J = 6.33$ Hz, 5-phenyl-H), 8.24 (d, 1H, $J = 6.6$ Hz, C_7-H), 9.75 (s, 1H, C_{10}-H). ^{13}C-NMR (DMSO-d_6) δ: 117.66, 124.09, 124.69, 127.75, 128.74, 129.80, 129.90, 129.96, 130.30, 131.67, 132.49, 132.80, 133.87, 134.44, 136.03, 136.33, 140.56, 142.84, 155.55, 157.10, 160.81. EIMS m/z 466 (M^+). Anal. calcd for $C_{23}H_{13}Cl_3N_4O$: C, 59.06; H, 2.80; N, 11.98. Found: C, 58.82; H, 2.77; N, 12.09.

*2-Amino-9-chloro-5-(4-chlorophenyl)-3-(2-chlorophenyl) pyrimido[4,5-c]quinolin-1(2H)-one (**2f**)*

Yield 33 %, mp 223–225 °C (DMF); ^{1}H-NMR (DMSO-d_6) δ: 5.94 (s, 2H, NH_2), 7.48–7.57 (m, 4H, 3-phenyl-H,

5-phenyl-H), 7.61–7.62 (d, 1H, $J = 5.22$ Hz, 3-phenyl-H), 7.68 (d, 1H, $J = 5.49$ Hz, 3-phenyl-H), 7.92 (dd, 1H, $J = 6.6$, 1.92 Hz, C_8-H), 8.06 (d, 2H, $J = 6.33$ Hz, 5-phenyl-H), 8.20–8.22 (m, 1H, C_7-H), 9.73–9.74 (m, 1H, C_{10}-H). ^{13}C-NMR (DMSO-d_6) δ: 118.71, 124.32, 125.08, 127.31, 128.04, 129.51, 130.25, 130.83, 131.46, 131.82, 132.00, 133.01, 134.24, 134.42, 134.80, 136.60, 140.88, 143.23, 155.92, 157.26, 160.88. EIMS m/z 466 (M^+). Anal. calcd for $C_{23}H_{13}Cl_3N_4O$: C, 59.06; H, 2.80; N, 11.98. Found: C, 58.94; H, 2.85; N, 12.02.

*2-Amino-3-(4-bromophenyl)-9-chloro-5-(4-chlorophenyl) pyrimido[4,5-c]quinolin-1(2H)-one (**2g**)*

Yield 57 %, mp 288–290 °C (DMF); ^{1}H-NMR (DMSO-d_6) δ: 6.09 (s, 2H, NH_2), 7.56–7.61 (m, 2H, 5-phenyl-H), 7.71–7.77 (m, 2H, 3-phenyl-H), 7.87–7.90 (m, 3H, 3-phenyl-H, C_8-H), 8.11–8.13 (m, 2H, 5-phenyl-H), 8.18 (d, 1H, $J = 6.6$ Hz, C_7-H), 9.69 (d, 1H, $J = 1.92$ Hz, C_{10}-H). ^{13}C-NMR (DMSO-d_6) δ: 117.52, 124.16, 124.38, 124.71, 127.82, 129.85, 130.92, 131.66, 132.30, 132.84, 133.33, 133.89, 134.47, 136.35, 140.64, 142.82, 155.98, 157.05, 160.86. EIMS m/z 510 (M^+). Anal. calcd for $C_{23}H_{13}BrCl_2N_4O$: C, 53.93; H, 2.56; N, 10.94. Found: C, 53.93; H, 2.60; N, 11.12.

*2-Amino-3-(3-bromophenyl)-9-chloro-5-(4-chlorophenyl) pyrimido[4,5-c]quinolin-1(2H)-one (**2h**)*

Yield 51 %, mp 275–276 °C (DMF); ^{1}H-NMR (DMSO-d_6) δ: 6.08 (s, 2H, NH_2), 7.47–7.51 (m, 1H, 3-phenyl-H), 7.57–7.63 (m, 2H, 5-phenyl-H), 7.74–7.76 (m, 1H, 3-phenyl-H), 7.91–7.93 (m, 2H, C_8-H, 3-phenyl-H), 8.12–8.15 (m, 3H, 5-phenyl-H, 3-phenyl-H), 8.21–8.23 (d, 1H, $J = 6.6$ Hz, C_7-H), 9.73 (d, 1H, $J = 1.65$ Hz, C_{10}-H). EIMS m/z 510 (M^+). Anal. calcd for $C_{23}H_{13}BrCl_2N_4O$: C, 53.93; H, 2.56; N, 10.94. Found: C, 53.95; H, 2.54; N, 11.09.

*2-Amino-9-chloro-5-(4-chlorophenyl)-3-(4-iodophenyl) pyrimido[4,5-c]quinolin-1(2H)-one (**2i**)*

Yield 46 %, mp 270–272 °C (DMF); ^{1}H-NMR (DMSO-d_6) δ: 6.08 (s, 2H, NH_2), 7.56–7.58 (m, 2H, 5-phenyl-H), 7.72–7.74 (m, 2H, 3-phenyl-H), 7.87–7.91 (m, 3H, 3-phenyl-H, C_8-H), 8.11–8.17 (m, 3H, 5-phenyl-H, C_7-H), 9.69–9.70 (m, 1H, C_{10}-H). EIMS m/z 558 (M^+). Anal. calcd for $C_{23}H_{13}Cl_2IN_4O$: C, 49.40; H, 2.34; N, 10.02. Found: C, 49.16; H, 2.39; N, 10.59.

*2-Amino-9-chloro-5-(4-chlorophenyl)-3-(4-methylphenyl) pyrimido[4,5-c]quinolin-1(2H)-one (**2j**)*

Yield 52 %, mp 276–277 °C (DMF); ^{1}H-NMR (DMSO-d_6) δ: 2.39 (s, 3H, CH_3), 6.10 (s, 2H, NH_2), 7.33 (d, 2H, $J = 6.03$ Hz, 3-phenyl-H), 7.59 (d, 2H, $J = 6.6$ Hz, 5-phenyl-H), 7.86–7.91 (m, 3H, 3-phenyl-H, C_8-H), 8.15 (d, 2H, $J = 6.57$ Hz, 5-phenyl-H), 8.19–8.21 (d, 1H, $J = 6.6$ Hz, C_7-H), 9.72 (d, 1H, $J = 1.65$ Hz, C_{10}-H). ^{13}C-NMR (DMSO-d_6) δ: 21.01, 117.00, 124.18, 124.58, 127.69, 128.33, 129.59, 130.19, 131.20, 131.57, 132.77, 133.69, 134.29, 136.36, 140.50, 140.67, 142.59, 156.65, 157.06, 160.75. EIMS m/z 446 (M^+). Anal. calcd for $C_{24}H_{16}Cl_2N_4O$: C, 64.44; H, 3.61; N, 12.53. Found: C, 64.47; H, 3.59; N, 12.80.

*2-Amino-9-chloro-5-(4-chlorophenyl)-3-(3-methylphenyl) pyrimido[4,5-c]quinolin-1(2H)-one (**2k**)*

Yield 51 %, mp 263–266 °C (DMF); ^{1}H-NMR (DMSO-d_6) δ: 2.40 (s, 3H, CH_3), 6.10 (s, 2H, NH_2), 7.35–7.43 (m, 2H, 3-phenyl-H), 7.59 (d, 2H, $J = 6.6$ Hz, 5-phenyl-H), 7.72–7.78 (m, 2H, 3-phenyl-H), 7.92 (dd, 1H, $J = 6.57$, 1.65 Hz, C_8-H), 8.16 (d, 2H, $J = 6.33$ Hz, 5-phenyl-H), 8.22 (d, 1H, $J = 6.6$ Hz, C_7-H), 9.74 (d, 1H, $J = 1.92$ Hz, C_{10}-H). EIMS m/z 446 (M^+). Anal. calcd for $C_{24}H_{16}Cl_2N_4O$: C, 64.44; H, 3.61; N, 12.53. Found: C, 64.23; H, 3.62; N, 12.36.

*2-Amino-9-chloro-5-(4-chlorophenyl)-3-(2-methylphenyl) pyrimido[4,5-c]quinolin-1(2H)-one (**2l**)*

Yield 37 %, mp 219–221 °C (DMF); ^{1}H-NMR (DMSO-d_6) δ: 2.22 (s, 3H, CH_3), 5.95 (s, 2H, NH_2), 7.32–7.54 (m, 6H, 3-phenyl-H, 5-phenyl-H), 7.88–7.91 (m, 1H, C_8-H), 8.02 (dd, 2H, $J = 6.4$, 1.8 Hz, 5-phenyl-H), 8.19 (dd, 1H, $J = 6.6$, 1.92 Hz, C_7-H), 9.70–9.74 (m, 1H, C_{10}-H). ^{13}C-NMR (DMSO-d_6) δ: 19.42, 118.14, 124.48, 125.03, 125.62, 127.96, 129.02, 129.72, 129.95, 130.24, 131.70, 132.86, 134.06, 134.65, 134.80, 136.17, 136.78, 140.95, 142.97, 157.45, 157.61, 160.62. EIMS m/z 446 (M^+). Anal. calcd for $C_{24}H_{16}Cl_2N_4O$: C, 64.44; H, 3.61; N, 12.53. Found: C, 64.19; H, 3.66; N, 12.35.

*2-Amino-9-chloro-5-(4-chlorophenyl)-3-(4-methoxyphenyl) pyrimido[4,5-c]quinolin-1(2H)-one (**2m**)*

Yield 53 %, mp 292–294 °C (DMF); ^{1}H-NMR (DMSO-d_6) δ: 3.85 (s, 3H, OCH_3), 6.13 (s, 2H, NH_2), 7.07 (d, 2H, $J = 6.6$ Hz, 3-phenyl-H), 7.61 (d, 2H, $J = 6.33$ Hz, 5-phenyl-H), 7.90 (dd, 1H, $J = 6.6$, 1.92 Hz, C_8-H), 7.99–8.01 (m, 2H, 3-phenyl-H), 8.16 (d, 2H, $J = 6.33$ Hz, 5-phenyl-H), 8.21 (d, 1H, $J = 6.57$ Hz, C_7-H), 9.73 (d, 1H, $J = 1.92$ Hz, C_{10}-H). EIMS m/z 462 (M^+). Anal. calcd for $C_{24}H_{16}Cl_2N_4O_2$: C, 62.22; H, 3.48; N, 12.09. Found: C, 61.95; H, 3.54; N, 12.08.

*2-Amino-9-chloro-5-(4-chlorophenyl)-3-(3-methoxyphenyl) pyrimido[4,5-c]quinolin-1(2H)-one (**2n**)*

Yield 49 %, mp 237 °C, dec. (DMF/EtOH); ^{1}H-NMR (DMSO-d_6) δ: 3.82 (s, 3H, OCH_3), 6.11 (s, 2H, NH_2), 7.11–7.13 (m, 1H, 3-phenyl-H), 7.41–7.45 (m, 1H, 3-phenyl-H), 7.51–7.53 (m, 2H, 3-phenyl-H), 7.56–7.59 (m, 2H, 5-phenyl-H), 7.87–7.90 (m, 1H, C_8-H), 8.13–8.20 (m, 3H, 5-phenyl-H, C_7-H), 9.70–9.71 (d, 1H, $J = 1.65$ Hz, C_{10}-H). EIMS m/z 462 (M^+). Anal. calcd for $C_{24}H_{16}Cl_2N_4O_2$: C, 62.22; H, 3.48; N, 12.09. Found: C, 61.97; H, 3.39; N, 12.07.

*2-Amino-9-chloro-5-(4-chlorophenyl)-3-(2-methoxyphenyl) pyrimido[4,5-c]quinolin-1(2H)-one (**2o**)*

Yield 38 %, mp 246–247 °C (DMF/EtOH); ^{1}H-NMR (DMSO-d_6) δ: 3.78 (s, 3H, OCH_3), 5.95 (s, 2H, NH_2), 7.11–7.19 (m, 2H, 3-phenyl-H), 7.54–7.56 (m, 4H, 3-phenyl-H, 5-phenyl-H), 7.89 (d, 1H, $J = 4.95$ Hz, C_8-H), 8.10 (d, 2H, $J = 6.06$ Hz, 5-phenyl-H), 8.19 (d, 1H, $J = 6.6$ Hz, C_7-H), 9.72 (s, 1H, C_{10}-H). ^{13}C-NMR (DMSO-d_6) δ: 55.86, 111.28, 117.46, 120.36, 123.88, 124.11, 124.66, 127.69, 129.73, 129.95, 131.57, 131.71, 132.72, 133.67, 134.28, 136.35, 140.68, 142.67, 155.81, 156.84, 157.02, 160.05. EIMS m/z 462 (M^+). Anal. calcd for $C_{24}H_{16}Cl_2N_4O_2$: C, 62.22; H, 3.48; N, 12.09. Found: C, 61.91; H, 3.40; N, 12.05.

*2-Amino-9-chloro-5-(4-chlorophenyl)-3-(3,4-dimethoxyphenyl)pyrimido[4,5-c]quinolin-1(2H)-one (**2p**)*

Yield 47 %, mp 282–283 °C (DMF/EtOH); ^{1}H-NMR (DMSO-d_6) δ: 3.81 (s, 3H, 4-OCH_3), 3.84 (s, 3H, 3-OCH_3), 6.18 (s, 2H, NH_2), 7.09 (d, 1H, $J = 6.06$ Hz, 3-phenyl-H), 7.59–7.70 (m, 4H, 3-phenyl-H, 5-phenyl-H), 7.89–7.91 (m, 1H, C_8-H), 8.16–8.21 (m, 3H, 5-phenyl-H, C_7-H), 9.72–9.73 (m, 1H, C_{10}-H). EIMS m/z 492 (M^+). Anal. calcd for $C_{25}H_{18}Cl_2N_4O_3$: C, 60.86; H, 3.68; N, 11.36. Found: C, 60.62; H, 3.72; N, 11.13.

*2-Amino-9-chloro-5-(4-chlorophenyl)-3-(3,5-dimethoxyphenyl)pyrimido[4,5-c]quinolin-1(2H)-one (**2q**)*

Yield 45 %, mp 294–295 °C (DMF/EtOH); ^{1}H-NMR (DMSO-d_6) δ: 3.80 (s, 6H, OCH_3), 6.12 (s, 2H, NH_2), 6.67–6.68 (m, 1H, 3-phenyl-H), 7.10–7.11 (m, 2H, 3-phenyl-H), 7.59 (d, 2H, $J = 6.03$ Hz, 5-phenyl-H), 7.78–7.79 (m, 1H, C_8-H), 8.16 (d, 2H, $J = 6.33$ Hz, 5-phenyl-H), 8.24 (d, 1H, $J = 7.17$ Hz, C_7-H), 9.75 (d, 1H, $J = 1.11$ Hz, C_{10}-H). EIMS m/z 492 (M^+). Anal. calcd for $C_{25}H_{18}Cl_2N_4O_3$: C, 60.86; H, 3.68; N, 11.36. Found: C, 60.60; H, 3.76; N, 11.70.

*2-Amino-9-chloro-5-(4-chlorophenyl)-3-(3,4,5-trimethoxyphenyl)pyrimido[4,5-c]quinolin-1(2H)-one (**2r**)*

Yield 51 %, mp 235–237 °C (DMF/EtOH); ^{1}H-NMR (DMSO-d_6) δ: 3.75 (s, 3H, 4-OCH_3), 3.84 (s, 6H, 3,5-di-OCH_3), 6.21 (s, 2H, NH_2), 7.36 (s, 2H, 3-phenyl-H), 7.60 (d, 2H, $J = 6.57$ Hz, 5-phenyl-H), 7.89 (d, 1H, $J = 6.87$ Hz, C_8-H), 8.17–8.22 (m, 3H, 5-phenyl-H, C_7-H), 9.72–9.73 (m, 1H, C_{10}-H). Anal. calcd for $C_{26}H_{20}Cl_2N_4O_4$: C, 59.67; H, 3.85; N, 10.71. Found: C, 59.60; H, 3.97; N, 11.02.

Biology

In vitro cytotoxicity

The new compounds were tested for their cytotoxic activity on the following human solid tumour cell lines: lung fibrosarcoma HT-1080 (American Type Culture Collection, Rockville, MD, USA), mammary adenocarcinoma MDA-MB-231 (ATCC), and colorectal adenocarcinoma HT-29 (European Collection of Cell Cultures, Salisbury, UK). All cells were routinely cultured in Dulbecco's minimal essential medium (DMEM) supplemented with penicillin (100 U/mL), streptomycin (100 μg/mL), and 10 % foetal bovine serum (media and antibiotics from Biochrom KG, Berlin, Germany) in an environment of 5 % CO_2, 85 % humidity, and 37 °C, and they were subcultured using a trypsin 0.25 %–EDTA 0.02 % solution. The cytotoxicity assay was performed by a modification of the MTT method (Metwally *et al.*, 2007a). Briefly, the cells were plated at a density of approximately 5,000 cells/well in 96-well flat-bottomed microplates, and after 24 h, the test compounds were added, appropriately diluted with DMSO. After a 72-h incubation, the medium was replaced with MTT (Sigma) dissolved at a final concentration of 1 mg/mL in serum-free, phenol red-free DMEM for a further 4-h incubation. Then, the MTT formazan was solubilized in 2-propanol, and the optical density was measured using an Infinite® M200 microplate reader (Tecan, Männedorf, Switzerland) at a wavelength of 550 nm (reference wavelength 690 nm). Doxorubicin hydrochloride (Sigma) was included in the experiments as positive control. The results represent the mean of three independent experiments and are expressed as IC_{50}, i.e. the concentration that reduced by 50 % the optical density of treated cells with respect to untreated controls.

Cell cycle analysis

Cell cycle analysis was performed following incubation of exponentially growing HT-1080 cells with the test substances (5 μM) for 36 h. Treated cultures were then

trypsinized, washed in phosphate-buffered saline (PBS), fixed in 50 % ethanol, and stained with an RNAse-containing propidium iodide solution (Metwally *et al.*, 2007a). DNA content was analysed on a FACS Calibur (Becton–Dickinson, San Jose, CA, USA) flow cytometer using the ModFit software (Verity Software House, Topsham, ME, USA).

In vitro inhibition of cellular tubulin polymerization

Exponentially growing HT-1080 cells (approximately 2×10^6 cells/dish) were treated with the test compounds (50 μM) for 24 h. Negative control cultures were treated with the corresponding concentration of vehicle (DMSO), while positive controls with either 1 μM colcemid (Biochrom) or 0.2 μM paclitaxel (Genexol®, Samyang Genex Corporation, Daejeon, Korea—kindly provided by Dr. M. Sagnou). Cultures were then trypsinized and washed in PBS, and polymerized cellular tubulin was separated from soluble tubulin dimers as described previously (Metwally *et al.*, 2007a). Briefly, cells were lysed in a buffer containing 20 mM Tris–HCl (pH 6.8), 1 mM $MgCl_2$, 2 mM EGTA, and 0.5 % Nonidet P-40 and protease and phosphatase inhibitor cocktails (Sigma) at room temperature and under low ambient light (Blagosklonny *et al.*, 1995). Supernatants were collected after centrifugation at 13,000×*g* for 10 min. The pellets were dissolved by heating for 5 min at 95 °C in a SDS–polyacrylamide gel electrophoresis (PAGE) sampling buffer and subjected to electrophoresis on a 10 % SDS-PAGE gel. After electrophoresis, the proteins were transferred to a PVDF membrane and subjected to Western analysis using an anti-α-tubulin monoclonal antibody and peroxidase-conjugated anti-mouse antibody (Sigma). Detection of immunoreactive bands was performed by chemiluminescence (ECL kit, Amersham Biosciences) according to the manufacturer's instructions on a Fujifilm LAS-4000 luminescent image analyser (Fujifilm Manufacturing Inc., Greenwood, SC, USA).

Results and discussion

All the target compounds were evaluated for in vitro cytotoxicity against two human cancer cell lines, namely lung fibrosarcoma HT-1080 and colon adenocarcinoma. The data are represented in terms of IC_{50} values (μM) which are the drug concentrations required for 50 % inhibition of net cell proliferation in comparison with untreated control cultures. Doxorubicin was used as a reference cytotoxic compound. Furthermore, the mechanism of action of the new compounds was investigated through flow cytometric cell cycle analysis and tubulin polymerization inhibition assay performed on a selected set of the most cytotoxic compounds.

Overall, cytotoxicity data revealed that two major conclusions can be initially drawn. Firstly, o-substituents bigger in size than a fluorine atom are not tolerated as evidenced by the relatively low cytotoxic activity of compounds **2c** (o-fluoro; 6.4 ± 1.8 μM) and **2o** (o-methoxy; 15.0 ± 3.6 μM) and lack of cytotoxicity of **2f** (o-chloro) and **2l** (o-methyl) up to 100 μM level when tested on the HT-1080 cell lines. Secondly, methoxy substituents, whatever was the number and pattern of substitution, showed more than eightfold higher cytotoxic selectivity for HT-1080 versus HT-29 cell lines. This finding was more obvious with the multimethoxy-substituted compounds **2q** and **2r**. While both compounds were inactive in the HT-29 cell line up to 100 μM level, they exhibited moderate cytotoxic activity against HT-1080 cells. Multiple methoxy substitution seemed to detract from cytotoxic activity in both cell lines tested. In fact, HT-29 cells were almost insensitive to multimethoxy-substituted compounds (**2p–r**). Interestingly, the trimethoxy-substituted compound (**2r**) had slightly lower cytotoxic activity (1.3 ± 0.8 μM) when compared to the m-methoxy analogue (**2n**; 1.0 ± 0.3 μM) against HT-1080 cell lines, but showed the highest cytotoxic selectivity for these cells versus HT-29 cell lines among the target compounds tested (Table 1).

For a more convenient discussion, the target compounds can be categorized into two distinct series: the 3-halophenyl and the 3-methyl/methoxyphenyl series. A clear-cut distinction in cytotoxicity pattern was shown by the 3-halophenyl series versus the 3-methyl/methoxyphenyl series. In the 3-halophenyl series, the p-halo substituents consistently displayed higher cytotoxic activity when compared to the m-halo substituents. For instance, the p-chloro analogue (**2d**) was more cytotoxic than its m-chloro counterpart (**2e**) in both cell lines tested. Interestingly, the p-iodo compound (**2i**) was found to be the most potent among the p-halo analogues displaying an IC_{50} of 1.1 μM against HT-1080 cell lines. In addition, this particular compound exhibited the highest cytotoxic selectivity for HT-1080 cells with an IC_{50} of 10.2 μM against HT-29 cells. In the methyl/methoxyphenyl series, however, m-substitution appeared to yield the most cytotoxic compounds. The m-methyl analogue (**2k**) was equipotent to its m-methoxy counterpart (**2n**) displaying 1.0 μM cytotoxic activity against HT-1080 cell lines. Both compounds were found to be less potent in the HT-29 cell lines with compound **2k** showing slightly higher IC_{50} value (5.7 ± 0.5 μM) as compared to **2n** (8.3 ± 4.2 μM). In both series, HT-1080 cells were generally more responsive to the cytotoxic effect of the target compounds as compared to HT-29 cells, in line with our previous observations (Metwally *et al.*, 2007a, 2013).

Table 1 In vitro cytotoxicity of the target pyrimido[4,5-*c*]quinolin-1(2H)-ones using the MTT assay (IC50 values in μM)

Compound	R	Cell line	
		HT-1080	HT-29
2a	4-F	1.8 (±0.2)	2.0 (±0.8)
2b	3-F	2.4 (±0.1)	5.8 (±1.8)
2c	2-F	6.4 (±1.8)	32.0 (±5.1)
2d	4-Cl	1.4 (±0.3)	2.4 (±0.2)
2e	3-Cl	5.3 (±0.8)	3.9 (±1.5)
2f	2-Cl	>100	NT[a]
2g	4-Br	1.9 (±0.2)	3.2 (±0.2)
2h	3-Br	3.4 (±0.4)	7.7 (±2.3)
2i	4-I	1.1 (±0.5)	10.2 (±1.0)
2j	4-CH3	2.6 (±1.0)	4.9 (±1.5)
2k	3-CH3	1.0 (±0.2)	5.7 (±0.5)
2l	2-CH3	>100	NT
2m	4-OCH3	24.6 (±9.2)	NT
2n	3-OCH3	1.0 (±0.3)	8.3 (±4.2)
2o	2-OCH3	15.0 (±3.6)	NT
2p	3,4-di-OCH3	8.6 (±5.3)	78.2 (±5.7)
2q	3,5-di-OCH3	6.2 (±1.4)	>100
2r	3,4,5-tri-OCH3	1.3 (±0.8)	>100
Doxo	–	0.0035 (±0.0001)	0.029 (±0.01)

The results represent the mean (±standard deviation) of three independent experiments and are expressed as IC50, the concentration that reduced by 50 % the optical density of treated cells with respect to untreated controls

[a] NT, not tested

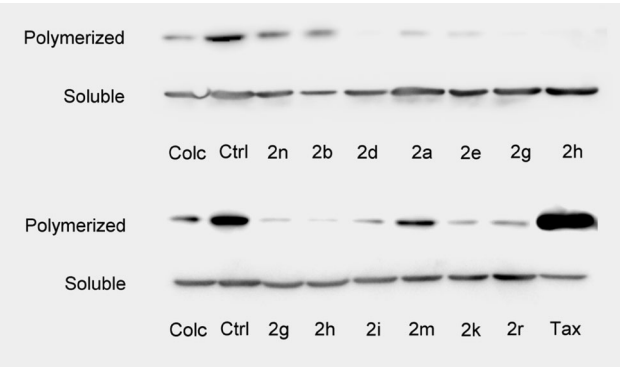

Fig. 2 Inhibition of cellular tubulin polymerization by test compounds compared to untreated cultures (Ctrl) and cultures treated with colcemid (Colc) or paclitaxel (Tax)

Table 2 Cell cycle phase distribution (%)

Compound	G_0/G_1	S	G_2/M
2a	40.74	21.27	37.99
2b	44.93	24.81	30.27
2d	37.30	22.41	40.29
2g	39.66	26.97	33.37
2i	44.10	26.86	29.04
2j	41.11	23.84	35.05
2k	41.79	28.88	29.33
2n	39.71	26.98	33.31
2r	45.68	26.91	27.41
Colcemid	8.57	12.73	78.71
Paclitaxel	7.67	24.21	68.12
Control	48.46	28.30	23.24

One out of two similar experiments is depicted

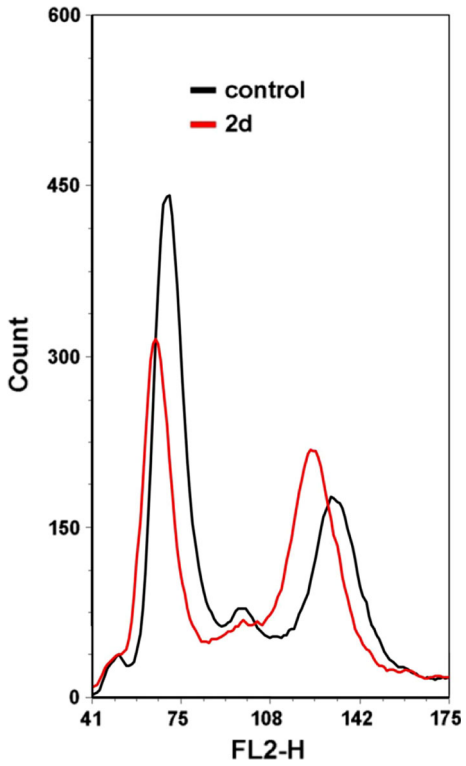

Fig. 3 Induction of G2/M arrest by test compound 2d compared to untreated cultures (control) as revealed by flow cytometric cell cycle analysis of HT-1080 cells

It is well documented that compounds interfering with microtubule dynamics induce apoptosis in cancer cells (Honore *et al.*, 2005; Dumontet, 2010; Amos, 2011). To examine the effect of our target compounds on cell cycle progression, the most cytotoxic compounds (IC_{50} in the range of 1.0–2.6 μM) were then tested for their effect on cell cycle through a flow cytometric analysis. This method highlights the effects of antimitotic compounds on the distribution of cells in specific phases of the cell cycle. To this end, the DNA content of HT-1080 cells after incubation with 5 μM compound for 36 h was analysed, through staining with propidium iodide followed by flow cytometry. Colcemid and paclitaxel were included as positive controls. All compounds tested were found to

arrest the cells in the G2/M phase of the cell cycle, in agreement with the hypothesis of action through interference with tubulin polymerization (Fig. 2). Cell cycle analysis data of the selected compounds are illustrated in Table 2. This hypothesis was pursued further using a tubulin polymerization assay, i.e. after incubation of HT-1080 cells for 24 h with the test compounds (50 μM) or with colcemid (1 μM) or paclitaxel (0.2 μM) used as control compounds, polymerized tubulin was separated from soluble tubulin and the two fractions were assessed by Western analysis. As shown in Fig. 3, all the tested compounds inhibited tubulin polymerization similarly to colcemid, in contrast to paclitaxel, which stabilizes and enhances tubulin polymerization.

Conclusion

We were able through the present investigation to shed some light on the SAR pattern of substitution at position 3 of the antimitotic pyrimido[4,5-*c*]quinolin-1(2*H*)-ones. Close inspection of biological results indicated that o-substitution of the 3-phenyl ring generally decreases cytotoxicity. On the other hand, p-substitution with a halogen or m-substitution with a methyl/methoxy group enhances cytotoxic activity. Multimethoxy substitution was not a positive contributor to cytotoxicity in both cell lines tested. In general, the target compounds were more cytotoxic to HT-1080 cells as compared to HT-29 cells. The most cytotoxic compounds arrested HT1080 cells in the G2/M phase and inhibited tubulin polymerization. Synthesis of new analogues with p-halophenyl and m-methyl/methoxyphenyl substituents is currently underway.

Acknowledgments The authors are grateful to the Scientific Research Administration, Zagazig University for providing the financial support for this work (24, 2012–2013).

References

Amos L (2011) What tubulin drugs tell us about microtubule structure and dynamics. Semin Cell Dev Biol 22:916–926

Blagosklonny M, Schulte T, Nguyen P, Mimnaugh E, Trepel J, Neckers L (1995) Taxol induction of p21WAF1 and p53 requires c-raf-1. Cancer Res 55:4623–4626

Downing K (2000) Structural basis for the interaction of tubulin with proteins and drugs that affect microtubule dynamics. Annu Rev Cell Dev Biol 16:89–111

Dumontet C, Jordan M (2010) Microtubule-binding agents: a dynamic field of cancer therapeutics. Nat Rev Drug Disc 9:790–803

Honore S, Pasquier E, Braguer D (2005) Understanding microtubule dynamics for improved cancer therapy. Cell Mol Life Sci 62:3039–3056

Jordan M, Wilson L (2004) Microtubules as a target for anticancer drugs. Nat Rev Cancer 4:253–265

Metwally K, Pratsinis H, Kletsas D (2007a) Pyrimido[4,5-c]quinolin-1(2H)-ones as a novel class of antimitotic agents: synthesis and in vitro cytotoxic activity. Eur J Med Chem 42:344–350

Metwally K, Aly O, Aly E, Banerjee A, Ravindra R, Bane S (2007b) Synthesis and biological activity of 2,5-diaryl-3-methylpyrimido[4,5-c]quinolin-1(2H)-one derivatives. Bioorg Med Chem 15:2434–2440

Metwally K, Khalil A, Pratsinis H, Kletsas D (2010) Synthesis, in vitro cytotoxicity, and a preliminary structure-activity relationship investigation of pyrimido[4,5-c]quinolin-1(2H)-ones. Arch Pharm Chem Life Sci 8:465–472

Metwally K, Khalil A, Pratsinis H, Kletsas D, Sallam A, El-Sayed K (2013) Structure–activity relationship investigation of methoxy substitution on anticancer pyrimido[4,5-c]quinolin-1(2H)-ones. Med Chem Res 22:4481–4491

Nogales E (2001) Structural insight into microtubule function. Annu Rev Biophys Biomol Struct 30:397–420

Schwartz E (2009) Antivascular actions of microtubule-binding drugs. Clin Cancer Res 15:2594–2601

Sorger P, Dobles M, Tournebize R, Hyman A (1997) Coupling cell division and cell death to microtubule dynamics. Curr Opin Cell Biol 9:807–814

Zhou J, Giannakakou P (2005) Targetting microtubules for cancer chemotherapy. Curr Med Chem Anticancer Agents 5:65–71